Carbonates and Evaporites (2019) 34:1799–1813
https://doi.org/10.1007/s13146-019-00528-w

ORIGINAL ARTICLE

Facies distribution, depositional environment, and diagenetic features of the Permian Jamal Formation, Central Iran basin

Fatemeh Aghajani[1] · **Mohsen Aleali**[1]

Accepted: 6 August 2019 / Published online: 20 August 2019

Abstract

The Permian Jamal Formation characterized as one of the most significant successions in the Central Iran basin and constitutes a thick section (as much as 180 m) of limestone, dolomitic limestone, and dolomite in southeastern Kharu village in Tang-e Sarve area. The facies analysis of Jamal Formation leads to the identification of 11 microfacies, which are attributable to shoal, lagoon, and tidal flat environments. Results from petrographic evidence as well as facies analysis demonstrate that the depositional environment of Jamal Formation in the studied area (Kharu village, East Tabas) exhibits the characteristics of a homoclinal carbonate ramp platform with the gentle slope. This platform is mainly composed of tidal flat, lagoon, and shoal sub-environments. According to facies frequency analysis, the lagoon environment accounts for the highest abundance of facies (48%), whereas tidal flat environment shows the least abundance (17%). Bioturbation, micritization, cementation, dolomitization, neomorphism, physical and chemical compaction, and fracturing are the most important diagenetic features.

Keywords Jamal Formation · Central Iran basin · Facies analysis · Depositional environments · Diagenetic features

Introduction

The Permian successions in Central Iran have been reported in two Kalmard and Tabas regions. In these areas, Permian deposits are characterized by the Jamal Formation. The Jamal Formation is one of the most important formations, situated in the Central Iran basin. In the type section (southern flank of Jamal anticline), Jamal Formation, with around 480 m thickness, is unconformably underlain by the Sardar Formation, while it is overlain by the lower Triassic Sorkh Shale Formation. Arefifard and Davydov (2005) and Arefifard and Isaacson (2009, 2011) are studied different sections of Permian successions in the central and east of Iran. They believed that in most places of Iran, Jamal Formation indicates carbonate lithology.

The studied section is located in eastern Iran near Tabas city. The Jamal Formation consists of a sequence of limestone, dolomitic limestone, and dolomite with a thickness around 180 m in the southeastern Kharu village in the Tang-e Sarve area (East of Tabas city). This section is marked by dolomitic limestone in the base, medium-to-thick bedded, foraminifera, algae-rich, dark limestone in the middle part, and a sequence of medium-to thick bedded, low fossiliferous dolomite in the upper part. Carbonate strata of the Jamal Formation in Central Iran can be correlated with the Ruteh and Nesen Formations in the Alborz basin (Brunet et al. 2009). Tang-e Sarve section, with an altitude, ranges up to 1662 m above sea level, enjoys the geographical coordination of 57 11 10E and 33 36 39N.

Stocklin et al. (1965) were the pioneers in introducing the Permian sediments named the Jamal Formation in Tabas region. Most explanations of the Jamal Formation were made by Rutner et al. (1968). In most studies, the age of the carbonate Jamal Formation sequence has been reported Early to Late Permian (e.g., Stocklin et al. 1965; Rutner et al. 1968; Kahler 1974, 1977; Jenny–Deshusses 1983; Partoazar 1992; Leven and Taheri 2003; Leven and Vaziri Moghaddam 2004; Arefifard and Isaacson 2011; Partoazar et al. 2014).

Since the introductory research of Stocklin et al. (1965), several scholars have been concerned with investigating the lithostratigraphy, biostratigraphy and general geology of the Permian successions in central and eastern Iran (e.g., Partoazar 1992, 1995; Senowbari-Daryan and Hamedani 2002; Taheri 2002; Ernst et al. 2006a, b, 2007, 2011; Senowbari-Daryan and Rashidi 2010; Ernst et al. 2006a, b, 2008, 2009a, b; Rashidi

✉ Mohsen Aleali
aleali.mohsen@gmail.com

[1] Department of Earth Sciences, Science and Research Branch, Islamic Azad University (IAU), Tehran, Iran

and Senowbari-Daryan 2010; Rigby et al. 2005; Arefifard and Davydov 2005; Yarahmadzahi 2011; Arefifard and Isaacson 2009, 2011; Partoazar et al. 2014; Leven and Gorgij 2006; Davidov and Arefifard 2007; Sotohian 2016), though few studies have been focused on the facies distribution and depositional environments of the Jamal Formation. Therefore, the ongoing research aims at identifying the types of facies, depositional environment, and diagenetic processes of the Jamal Formation in Tang-e Sarve (Tabas area).

Geological setting

Iran has been divided into several structural units, each characterized by a relatively unique record of tectonic, stratigraphy, metamorphism, magmatic activities, sedimentary features, and overall geological structure (Aghanabati 2004). Central Iran seems to form a triangle in the interior part of Iran (Takin 1972; Stocklin 1977; Alavi 1991). This middle triangle (Nogole sadat 1978) is part of the Cimmerian continent (Sengor 1984) that has rifted away from the north Gondwana in the late Paleozoic (Scotese and Langford 1995; Dercourt et al. 1993). The Central Iran domain (named by Stocklin 1977) has experienced several tectonics events, periods of orogeny, magmatism, and metamorphism from Precambrian to recent age. Alavi (1991); Alavi et al. (1997) propounds the view that long strike-slip dextral faults (Kalmard, Posht-e-Badam, Kuhbanan, and Nayband) have divided Central Iran province into four sub-blocks including Tabas (TB), Yazd (YB), Posht-e-Badam (PBB), and Lut (LB). The Tang-e Sarve (target section) is located in the Tabas block (Fig. 1). The Tabas area is laid between two very active faults, namely, Nayband (in the east) and Kalmard-Kuhbanan (in the west). This block is separated from Tabas block by Nayband fault (Stocklin et al. 1965) and also, isolated from Yazd block by the Kuhbanan and Kashaneh-Kalmard curved faults (Alavi 1991). Providing mobile conditions of Tabas area, these active faults formed complicated Tectono-sedimentary evolutions throughout the Phanerozoic (Fig. 2). According to the random sampling of brachiopods, conodonts, ammonoids, and fusulinids, the Jamal Formation tends to date back to the Artinskian stage (Permian age). Aghanabati (1977) determines an Early to a Late Permian age for the Jamal Formation. Arefifard and Isaacson (2011) studied several sections of the Jamal strata and eventually attributes it to the Artinskian–early Wuchiapingian.

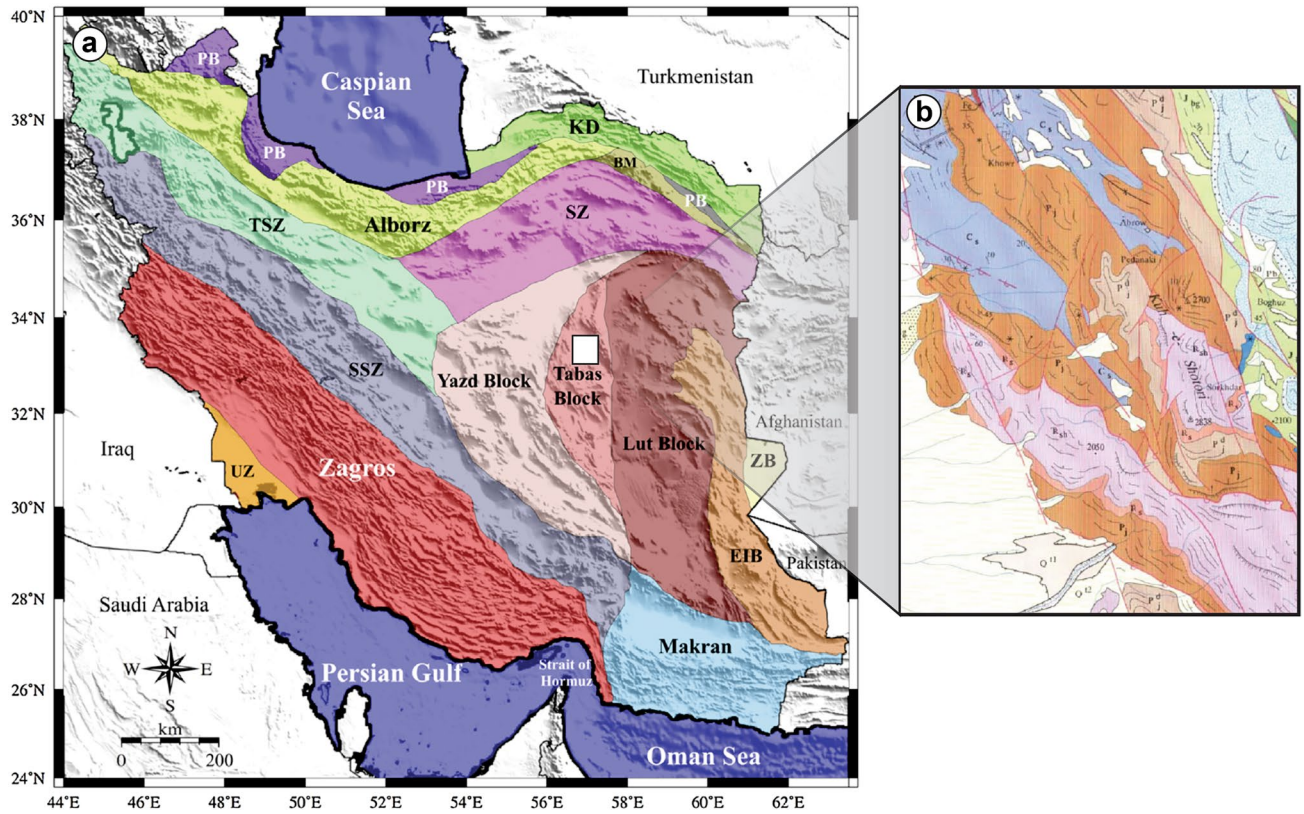

Fig. 1 **a** Structural map of Iran (modified after Aghanabati 2004; Hessami et al. 2006; Reilinger et al. 2006; Naimi-Ghassabian et al. 2015; Mousavi 2017). Abbreviations; UZ, unfolded zone; ZB, Zabol block; EIB, East Iranbelt; SSZ, Sanandaj–Sirjan zone TSZ, Tabriz–Saveh zone; SZ, Sabzevar Zone; KD, Kopeh-Dagh; BM, Binalud mountain range and PB, Paleo-Tethyan basin. **b** Geological map of Tang-e Sarve section (at 1.250000 scale) (Stocklin and Nabavi 1969)

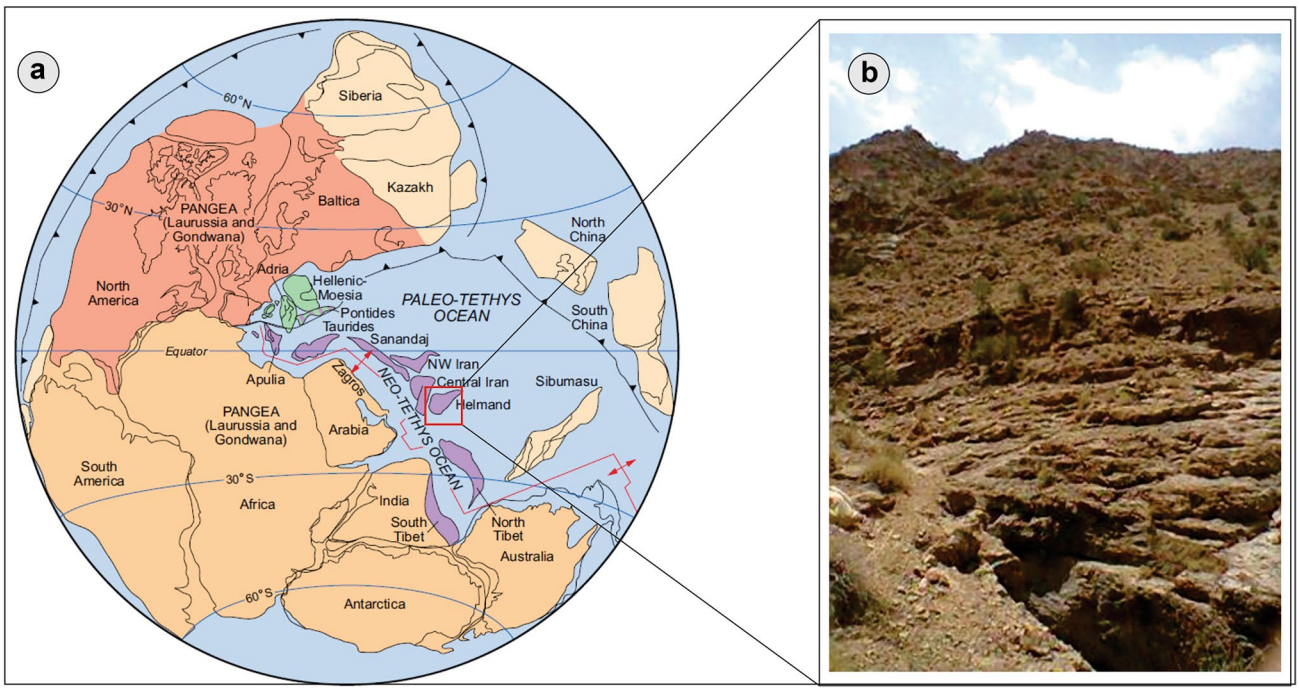

Fig. 2 **a** Plate-tectonic reconstruction of the late Permian (Lopingian) time (modified after Torsvik and Cocks 2004; Ruban et al. 2007). **b** General view of the Jamal Formation section (Tang-e Sarve)

Materials and methods

In this study, a detailed facies, diagenesis, and depositional system analysis is carried out in one section of the Jamal Formation in the Tang-e Sarve area in southeastern Kharu village (eastern Tabas City). The section is described on the basis of lithology, bedding, and sedimentary surfaces as well as facies compositions. Around 100 thin sections are sampled from the non-weathered surface and then analyzed by polarized microscope to define various microfacies types. Textural classification and carbonate facies-type identification are also conducted using Dunhum (1962) and Embry and Klovan (1971) classifications. Flugel (2010) and Dunhum (1962) are applied to the depositional environment determination and facies analysis (fauna and lithology).

Facies and depositional environment

According to petrographic studies, 11 microfacies that belong to three different facies belts including tidal flat, lagoon, and shoal environments are identified. These facies belts from the sea to the coast include.

Shoal facies belt (A)

This facies belt consists of four facies including FA1, FA2, FA3, and FA4.

Bioclast–intraclast grainstone (FA1)

The matrix of this facies is covered by light-colored sparry calcite. The skeletal allochems contain bivalves and echinoid/crinoid fragments, green algae, and bryozoan in addition to benthic foraminifera such as *Misellina* and *Staffella, Pseudoschwagerina*. The non-skeletal allochems are also peloid (rare) and intraclast. Comparable to RMF8 in Flugel (2010) (Fig. 3a), this facies also undergoes various diagenesis processes such as dolomitization (in the form of medium crystals), micritization, cementation, neomorphism, fracturing, and microfracturing (fractures are filled by cement).

Bioclast grainstone (FA2)

The bioclast grainstone mostly consists of skeletal components surrounded by sparry cement (calcite). The skeletal grains comprise of bivalve fragments, bryozoan, dasycladacean green algae, and benthic foraminifera such as *Miliolida, Pachyphloia,* and *Fusulina*. Intraclast is the subordinate grain. The micritizied margin of constituents (grains) represents the activity of such micro-organisms as microbes and endolithic algae in this part. The allochems are relatively well rounded and sorted. Exhibiting the characteristics of RMF27 in Flugel (2010) (Fig. 3b), this facies is influenced by various diagenesis processes such as dolomitization, micritization, cementation, recrystallization, and fracturing.

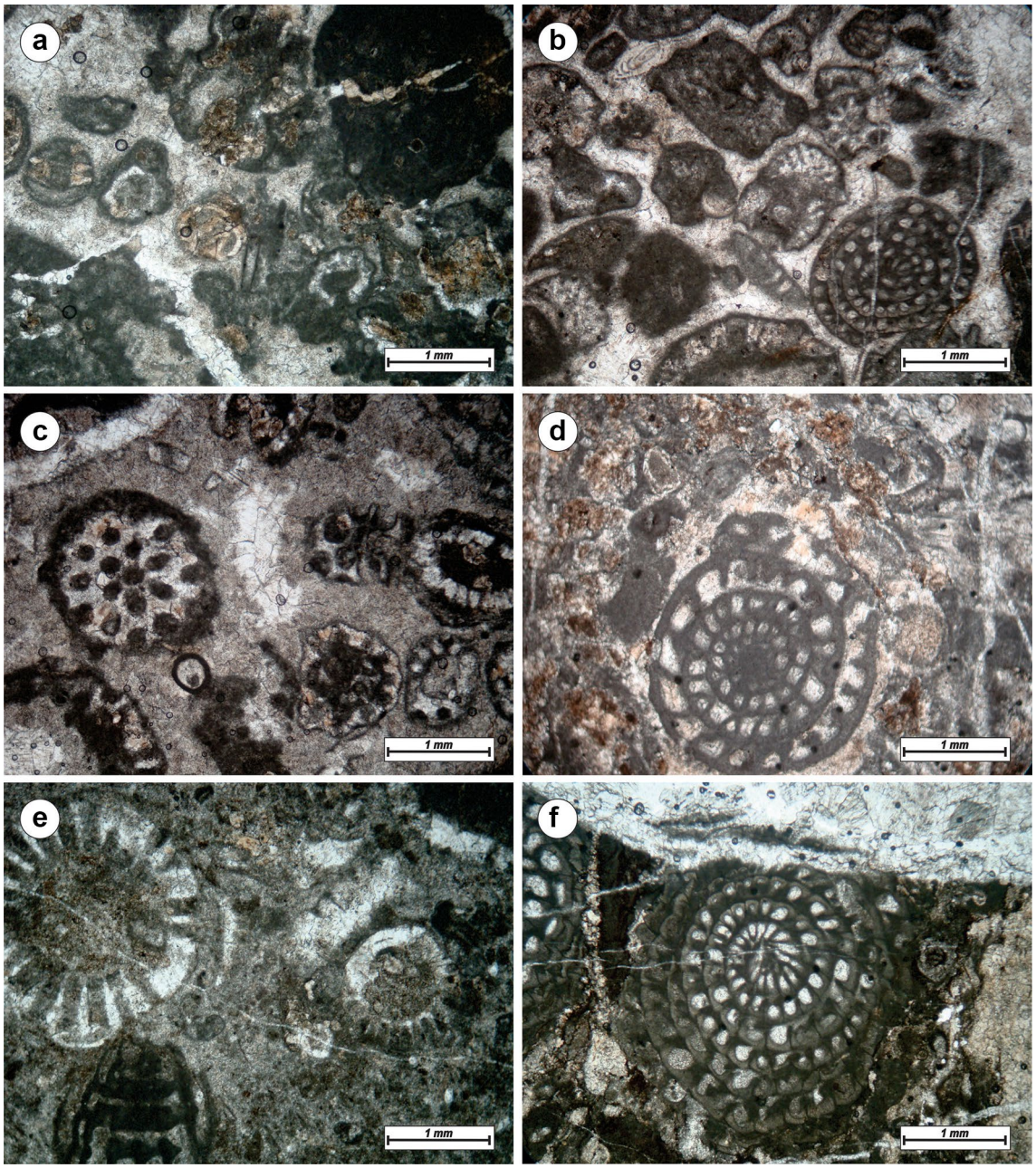

Fig. 3 Microfacies types of the Jamal Formation. **a** Bioclast–intraclast grainstone (FA1). **b** Bioclast grainstone (FA2). **c** Dasycladaceae bioclast packstone to grainstone (FA3). **d** Bioclast benthic foraminifera packstone to grainstone (FA4). **e** Dasycladaceae bioclast packstone (FB1). **f** Large benthic foraminifera packstone (FB2)

Dasycladaceae bioclast packstone to grainstone (FA3)

This facies contains microspar-to-sparite matrix as well as bioclast fragments specially dasycladaceae green algae (abundant). Dasycladaceae green algae (especially *Mizzia* sp.) comprise approximately 40–65% of grains in various size. The other skeletal constituents are echinoid and bivalve debris and benthic foraminifera such as *Miliolida, Fusulina,* and *Schwagerina*. Cementation, micritization, dolomitization, and fracturing account for major diagenetic features (Fig. 3c).

Bioclast benthic foraminifera packstone to grainstone (FA4)

This facies is overlain by a dark micritic to a light sparry matrix. Bivalves and echinoid fragments, dasycladaceae

green algae, and benthic foraminifera (such as *Pseudoschwagerina*) are the chief skeletal allochems. Major portion of the grains are crushed and micritized. These grains are of the medium-to-coarse size, but not sorted and rounded. Besides micritic grains, sorted and rounded peloid grains are minor grains. In some cases, replacement of non-texture selective dolomite has destroyed the fabric of grains. The most important diagenesis processes are dolomitization, equant calcite cement, micritization, and physical compaction as well as stylolite (uncommon). This facies is comparable to RMF26 in Flugel (2010) (Fig. 3d).

Interpretation

The facies belt characteristics point to the deposition of facies in the high-energy, disturbed environment. In general, the grain-supported nature, lack of mud (or low mud contents), medium-to-large grain size, and type of fauna refer to high-energy turbulent shoal environment (Wilson 1975; Tucker and Wright 1990; James and Jones 2015). In facies FA1 and FA2, because of current and wave dominant conditions, micrite is thoroughly washed and replaced by sparry calcite cement, which is referred to high-energy central to seaward shoal environments (Read 1985; Flugel 2010; Aleali et al. 2013). The packstone-to-grainstone texture, weak sorted, and rounded grains in facies FA3 and FA4 reveal that these facies are formed at the leeward part (lagoon side) of shoal environment, where the level of energy is lower than other parts of the shoal.

Lagoon facies belt (B)

This facies belt comprises of five facies including FB1, FB2, FB3, FB4, and FB5.

Dasycladaceae bioclast packstone (FB1)

The matrix of dasycladaceae bioclast packstone is dark-colored micrite (carbonate lime mud). The main bioclastic allochems contain dasycladaceae green algae (*Mizzia* sp.), bryozoan, bivalve, and echinoid particles and benthic foraminifera such as *Paleotextularia* and *Miliolida*. In addition to bioclastic fragments, moderate-to-well-sorted and well-rounded peloid grains are observed (less than 10 percent). Most of the skeletal components are neomorphed by sparry calcite. Different diagenetic processes such as selected dolomitization, cementation, micritization, neomorphism as well as fracturing and low-amplitude stylolite are identified. This facies is equivalent to RMF17 in Flugel (2010) (Fig. 3e).

Large benthic foraminifera packstone (FB2)

This grain-supported facies is characterized by a richness of large benthic foraminifera. The main foraminifera grains include *Misellina, Neofusalinella, Palotextolaria, Schwagerina,* and *Armonia.* The size of foraminifers ranges from 0.7 to 2.5 mm, constituting around 20–40% of grains. In addition to foraminifers, a limited amount of green algae, bivalve, and echinoid, gastropod and peloids is present. The grains are surrounded by dark-colored micrite.

Stylolites, filled by clay mineral, are founded. In certain thin sections, matrix and foraminifer chambers are replaced by dolomite (selective dolomitization). Two generations of fracturing and microfracturing filled by microcrystalline calcite cement are perceived. This facies is similar to RMF13 in Flugel (2010) (Figs. 3f, 4a).

Bioclast packstone (FB3)

The matrix of this facies is mainly coated by micrite, yet there is sparry cement in some small parts. The main skeletal grains are composed of benthic foraminifera (such as *Lunucammina, Pachyphloia, Paleotextularia,* and *Staffella*), green algae, gastropoda along with bivalve and echinoid/crinoid fragments (spine and plates). Non-skeletal fragments include peloid and oncoid (rare). Bioturbation is prevalent, and most of the grains are surrounded by a micritic envelope. Dolomitization is one of the diagenesis processes, which have selectively and dispersedly replaced matrix and grains (spatially around fracture and stylolites). In other parts, dolomite crystals are present around or within foraminifer chambers. Syntaxial overgrowth calcite cement is spread out around the echinoid/crinoid debris. This facies is comparable to RMF7 in Flugel (2010) (Fig. 4b).

Peloid bioclast packstone (FB4)

Peloid bioclast packstone mostly consists of skeletal components and peloid, encircled by a dark lime mud (micrite). The major skeletal components comprise of bivalve and echinoid/crinoid fragments, gastropoda, bryozoan, and benthic foraminifera such as *Endothyra, Miliolida, Lunucammina, Staffella,* and *Pachypholoia.* Peloid is the only non-skeletal allochem. The grains undergo micritization due to the effects of micro-boring organisms. The main diagenetic features are bioturbation, micritization, stylolite, fracturing, equant calcite cement, and dolomitization (coarse euhedral dolomite). This facies is analogous to RMF20 in Flugel (2010) (Fig. 4c).

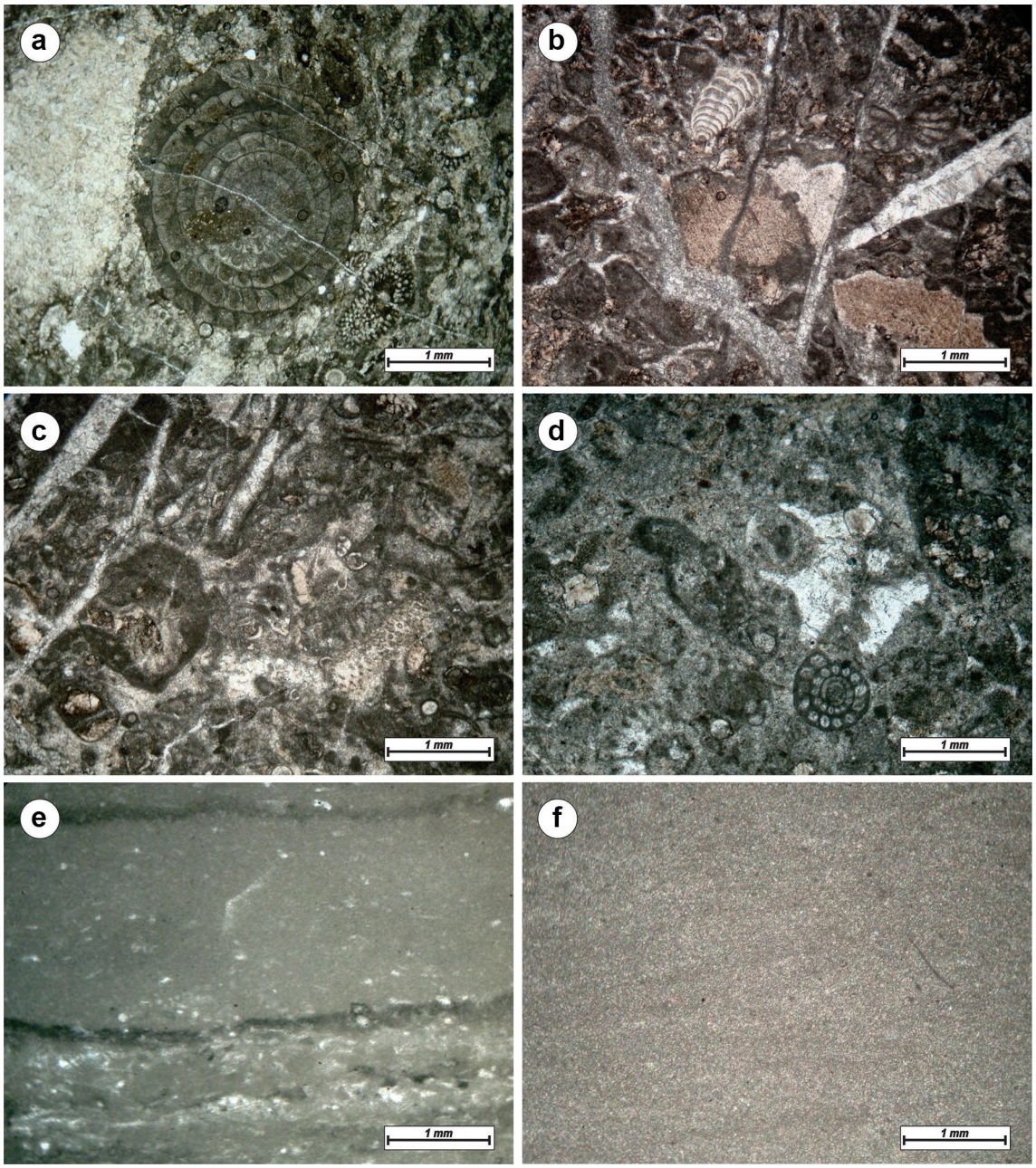

Fig. 4 Microfacies types of the Jamal Formation. **a** Large benthic foraminifera packstone (FB2). **b** Bioclast packstone (FB3). **c** Peloid bioclast packstone (FB4). **d** Bioclast wackestone (FB5). **e** Stromatolite boundstone (FC1). **f** Dolomudstone (FC2)

Bioclast wackestone (FB5)

The Bioclast wackestone is mostly made of skeletal particles, embraced by fine-grained lime mud (micritic) background. The grains are mainly composed of benthic foraminifera (such as *Miliolida, Endothyra,* and *Neoschwagerina*), bivalve, and echinoid debris and dasycladaceae green algae. Moreover, semi-sorted and rounded peloid grains are found. The major diagenetic processes are micritization, bioturbation, neomorphism, fracturing (filled by calcite cement) stylolite, and dolomitization (medium-to-fine crystalline dolomite). This facies is comparable to RMF17 in Flugel (2010) (Fig. 4d).

Interpretation

Given the paleontological characteristics (subtidal fauna) of sedimentary texture (abundance of lime mud), this facies belt belongs to the sub-tidal shallow marine environment. Packstone-to-wackestone texture along with abundance of

carbonate mud (micritic texture), the existence of lagoon fauna, particularly porcelaneous-wall benthic foraminifera and dasycladacean green algae, and the plenty of peloid grains point to the low energy restricted lagoon environment (Wilson 1975; Shinn 1968; Tucker and Wright 1990; Geel 2000; Bachmann and Hirsch 2006; Brandano et al. 2010; Arefifard and Isaacson 2011; Lasemi et al. 2012). Dasycladacean green algae are most abundant in relatively shallow, protected lagoons (Wray 1977; Flügel 1991; Rashidi and Senowbari-Daryan 2010; Senowbari-Daryan et al. 2011). Bioturbated and micritized facies of this facies belt mentioned to slow sedimentation in the calm sedimentary environment (especially lagoon)(Bathurst 1966; Longman 1980; Bottjer and Droser 1994; Bromley 1996; Patterson and Walter 1994; Aleali et al. 2013).

Tidal flat facies belt (C)

This facies belt consists of two facies including FC1 and FC2.

Stromatolite boundstone (FC1)

Stromatolite boundstone is thin-laminated bio-chemical facies of the Jamal Formation, which is formed from alternative light and dark layers. This facies is created by the growth of one-celled organisms (such as cyanobacteria) and the trapping sediments in the shallow water tidal flat environments. The structure of this facies is thin, flat or dome-shaped laminated. Besides Stromatolite boundstone, Keystone, bird's eye fabrics, and the small amount of peloid and shell fragments (less than 10%) are present. This facies is similar to RMF23 in Flugel (2010) (Fig. 4e).

Dolomudstone (FC2)

The matrix of this mud-supported facies is dark lime mud (micrite), though most parts of the microfacies are 80–100% dolomitic, thereby coining the term dolomudstone to name the facies. The dolomite anhedral crystals vary in size from 5 µm (very fine crystals) to 15 µm (fine crystals). In some thin sections, fenestral, mud crack, and bioturbation fabrics are seen. This facies is analogous to RMF22 in Flugel (2010) (Fig. 4f).

Interpretation

This facies group is identified as the shallowest facies belt of the Jamal Formation and classified into two microfacies types (Stromatolite boundstone and dolomudstone). Most researchers believe that Stromatolite boundstone is formed as a result of microbial activity, along with the process of stabilizing and trapping particles in shallow and low energy environments (e.g., Logan et al. 1964; Riding 1999, 2000; Warren 2006; Pratt 2010). Stromatolites are usually formed and maintained in the intertidal to upper supratidal zone (e.g., Shinn 1983; Alsharhan et al. 2003; Warren 2006; Palma et al. 2007; Flugel 2010; Bosence et al. 2015). Taking into the account the lack of marine skeletal grains, the abundance of fine dolomite crystals (dolomicrite), the presence of fenestral and bird's eye fabrics and mud-supported nature, FC2 belongs to the tidal flat environment (spacially intertidal zone). Fenestral and bird's eye fabrics are the result of gas outflow from sediments, hence referring to the intertidal subenvironment (Shinn 1983, 1986; Korngreen and Benjamini 2010; Rankey and Berkeley 2012).

Depositional model of the Jamal Formation

According to microfacies types, facies interpretations, and vertical and horizontal facies changes, carbonate depositional environment of the Jamal Formation is characterized as a homoclinal carbonate ramp with low angle (Fig. 5), which is confirmed by gradual shallowing trend of facies (from the barrier to the tidal flat sub-environment), the absence of enormous barrier reef, lack of calciturbidite, and talus and slumping sediments (Flugel 2010; Pomar 2001; Burchette and Wright 1992; Tucker and Wright 1990). This ramp is made up of various sub-environments including tidal flat, lagoon, and shoal (Fig. 5). Records of homoclinal carbonate ramp of the Jamal Formation in central Iran have been documented by other authors (e.g., Arefifard and Davydov 2005; Arefifard and Isaacson 2011; Sotohian 2016). In compliance with the obtained results, Arefifard and Isaacson (2011) support the notion that Permian deposits of the Jamal Formation in the Shirgesh and Shotori areas are deposited on a homoclinal carbonate ramp that demonstrates a deeper water facies in the northern parts (Bagh-e-Vang section) relative to the southern parts.

Based on the surface wave base (SWB, FWWB), ramps can be divided into three parts: inner, middle, and outer ramp. Accordingly, the Jamal Formation represents the conditions of the inner and middle ramp, such that the inner ramp is highly dominant in this area due to the higher thickness of lagoon and shoal facies.

Frequency analysis of facies illustrates that the lagoon environment has the highest abundance of facies (48%), while the tidal flat environment has the least abundance (17%) (Fig. 6a). The most frequent facies is bioclast packstone (FB3) with 19% frequency, whereas the Stromatolite boundstone (FC1) shows the least abundance with almost 4% frequency (Fig. 6b).

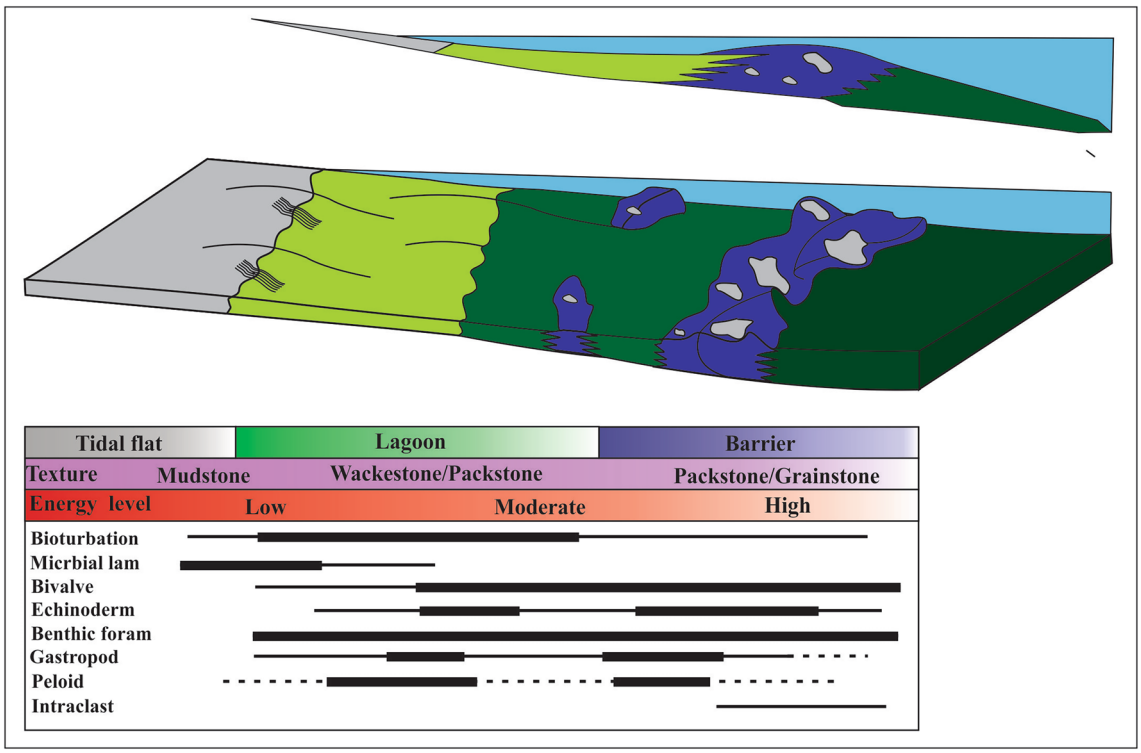

Fig. 5 Schematic diagram of a carbonate ramp platform setting that illustrates the depositional model of the Jamal Formation. Distribution of microfacies belts in carbonate ramp together with the components of the facies is observed

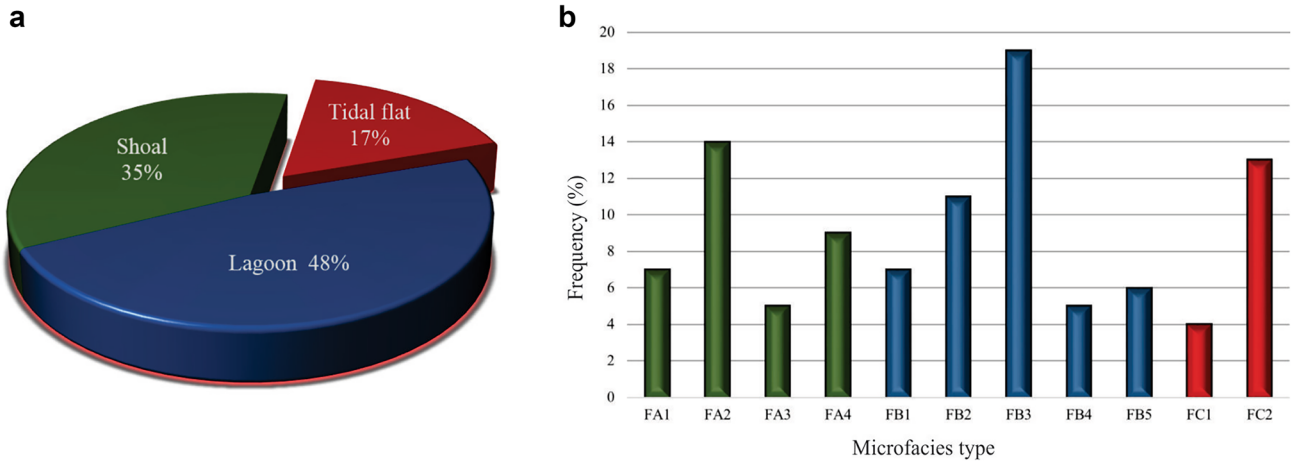

Fig. 6 Frequency diagrams showing frequency of facies belts and types of the Jamal Formation. **a** Pie diagram showing facies belts frequency. **b** Column diagram illustrating facies-type frequency

Diagenesis processes of Jamal Formation

According to the microscopic examination, the main diagenetic processes of the Jamal Formation are bioturbation, micritization, cementation, neomorphism, dolomitization, fracturing, chemical compaction, and physical compaction.

To determine the diagenetic processes and describe diagenetic environments, valid diagenetic concepts are employed (e.g., Harris et al. 1985a, b; James and Choquette 1983, 1990a, b; Longman 1980; Tucker and Bathurst 1990; James 1991; Flugel 2010; Moore and Wade 2013; James and Jones 2015).

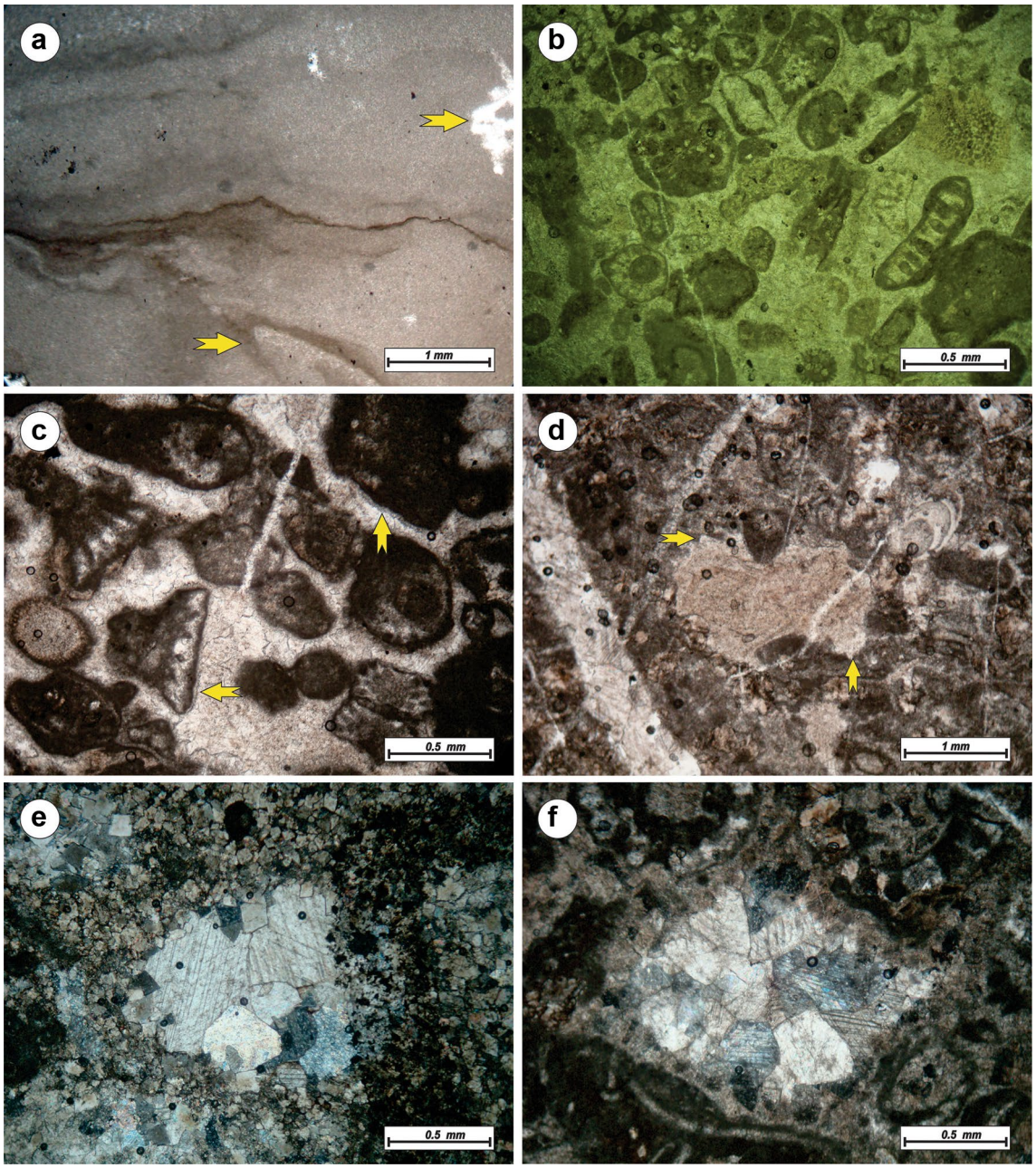

Fig. 7 Diagenetic features of the Jamal Formation. **a** Bioturbation of tidal flat dolomudstone, note the yellow arrows. **b** Micritization marked by dark micritic envelope around skeletal grains. **c** Isopachous bladed calcite cement occurs in the form of equal and parallel crystals around grains. **d** Syntaxial overgrowth calcite cement marked by clear rim cement around echinoderm plate **e** Drusy calcite cement with increasing in crystals size toward the center of void (ppl). **f** Equant calcite cement consists of cement crystals of the same size (ppl)

Bioturbation

Bioturbation is basically a syn-depositional process, whereby organisms disturb the sediments in the early of diagenetic history (Bromley 1994). Bioturbation is one of the most prevalent processes of subtidal zones and frequently occurs in the marine phreatic environment (Flugel 2010; Demicco and Hardie 1994). Burrowing and boring created by benthic creatures are the most significant forms of bioturbation in the Jamal Formation. This process is characterized by a change in the color of the matrix, deforms the original depositional texture,

and creates cavities and corrosion in the grains. Bioturbation is mainly developed in tidal flat and lagoon mud-supported facies (FB and FC facies belts) (Fig. 7a).

Micritization

The micritization is marked by dark micrite rims around the carbonate grains (Fig. 7b). Micritization has influenced the skeletal and non-skeletal fragments in tidal flat, lagoon, and shoal environments. This process creates a dark micrite envelope (Bathurst 1966) around the grains, particularly around the skeletal fragments. The thickness of the envelopes varies from a few µm to about 100 µm. A growing body of research has provided ample support for the assertion that micritization mainly occurs in the marine diagenetic environment (e.g. Bathurst 1966, 1989; Kobluk and Risk 1977; Reid et al. 1992), especially in the stagnant marine phreatic zone (Longman 1980).

Cementation

Cementation is the process of precipitation of mineral matter (cements) in pores within sediments or rocks. As one of the several diagenetic processes (such as physical and chemical compaction and mineral replacement) known as constructive diagenesis, cementation is an important diagenetic event that produces progressive porosity reduction and lithification of sedimentary strata with increasing age and/or depth of burial (Middleton et al. 2003). The Jamal Formation contains various types of cements as follows.

Bladed calcite cement

This cement is composed of isopachous blades at the external edge of the grains and within cavities (spacially skeletal cells and foraminifer chambers), and is usually followed by equant calcite cement. It is mainly observed in the high-energy barrier facies (FA1–FA4) (Fig. 7c). Bladed isopachous calcite cement is interpreted as marine (Bricker 1973; James and Choquette 1983; Sandberg 1985; Hird and Tucker 1988) and meteoric (Longman 1980) diagenetic environments.

Syntaxial overgrowth calcite cement

This cement is marked by overgrowth of clear rim cement in optical continuity with large monocrystalline host grains. It is substrate-controlled overgrowth cement around host grains made by a single crystal (Flugel 2010). The main mineralogy of syntaxial overgrowth cement is high-mg calcitic (Maliva 1995; Meyers 1991). The near-surface marine diagenetic syntaxial overgrowth cement marine is easily recognizable due to its cloudy appearance and presence of inclusion. Syntaxial overgrowth cement is developed around skeletal components with monocrystalline structure (specially echinoderm and crinoid fragments) (Fig. 7d). In addition, this cement is clear and is most likely to form in the meteoric or/and burial environments.

Drusy calcite cement

Drusy calcite cement is usually formed in the space between the grains, skeletal pore spaces, along with the fractures and within the mold porosities resulting from dissolution. This cement is characterized by equant to extended and euhedral-to-subhedral crystals. One of the most important characteristics of this cement is to increase the size of crystal towards the center of pore space (holes, cavities, or vugs). It is easily recognized in the facies of the Jamal Formation as the size of its crystal increases towards the center of pores (Fig. 7e). The size of the crystals is protean, mainly greater than 15 microns to a few millimeters. This cement is usually formed within shallow meteoric and burial environments (Choquette and James 1987; James 1991; Flugel 2010).

Equant calcite cement

Crystals of equant cement with different sizes form in the pores, intergranular spaces, and skeletal chambers. Crystals range in size from 0.1 to 2 mm. This cement can be found in the form of mosaics with anhedral, equant, and crystalline calcite. Equant cement usually forms within marine, meteoric, or burial environments (Tucker 2001; Scoffin 1988; Harris et al. 1985a; Pierson and Shinn 1985; Schneidermann and Harris 1985; Longman 1980). This cement can also be the result of the crystallization of the previous cements (Flugel 2010). This cement is not very common in the studied sequence (Fig. 7f).

Dolomitization

The dolomitization of carbonate rocks is one of the most common processes. Euhedral, coarse-grained dolomites, which fill pores as cement, are very common in the facies. Depending on the size of pores, crystals may increase in size from the walls towards the center of pores and fractures and are mostly found within lagoon and shoal environments. In some parts of the Jamal Formation, dolomitization is texture selective (fabric retentive dolomite) and affects some fabrics such as skeletal grains or matrix (Fig. 8b); in other parts, dolomitization is non-texture selective (fabric destructive dolomite) and destroys the fabric of rock (Fig. 8a).

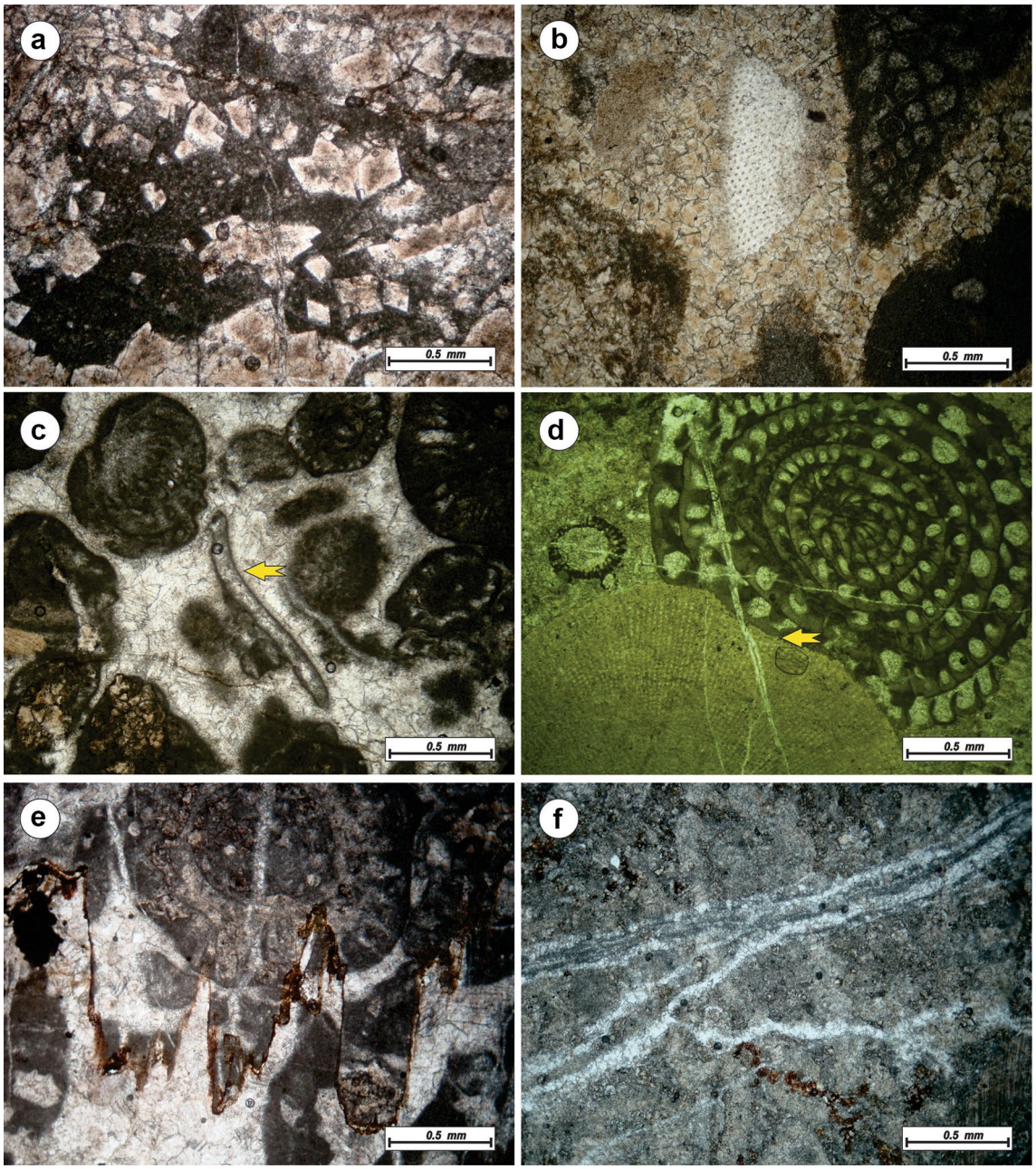

Fig. 8 Diagenetic features of the Jamal Formation. **a** Pervasive fabric destructive dolomite, note to the euhedral dolomite crystals with easily known and sharp rhombohedral (with acute-angled triangle crystal forms). **b** Carbonate matrix replaced by fabric retentive dolomite. **c** Bivalve fragment with dark micritic ring replaced by calcite crystals. **d** Concave–convex and sutured contact between two bioclastic grains. **e** Chemical compaction (stylolite filled by iron oxide). **f** Irregular anastomosing calcite-filled fractures

Neomorphism (recrystallization)

The transformation of aragonite and high-Mg calcite grains and mud-to-low-Mg calcite is one of the most important processes in carbonate diagenesis, commonly known as neomorphism. This process is mostly reported within grain-supported facies of the Jamal Formation and is characterized as a neomorph fabric (Fig. 8c). In most parts, increasing neomorphism destroys the internal fabric of the grains and substitutes them with calcite. In these cases, original (early) texture detection is very difficult or sometimes is impossible. Recrystallization changes the shape and size of crystals and ruins the fabric of grains. Previous studies put forward the view that this process is likely to occur in the meteoric (e.g., Pingitore 1976) and burial (e.g., Kendall 1975) diagenetic environments.

Physical compaction

Physical compaction creates various structural within mud-supported and grain-supported deposits. The main effects in mud-supported deposits include thinning and bending of laminations and destroying such structures as fenestral and burrow fabrics. The major physical compaction effects in grain-supported sediments are characterized by the deformation of the grain (such as peloids and skeletal fragments), fracturing, compressing, and cracking grains. Furthermore, compaction creates convex–concave contact between some of the grains (Fig. 8d). Physical compaction is commonly found within tidal flat, lagoon, and shoal facies. This process has been reported in the marine and burial environment (Moore 1989).

Chemical compaction (stylolite)

Stylolites are irregular, suture-like contacts produced by differential vertical movement under pressure accompanied by the solution. They are marked by irregular and interlocking penetration on two sides: columns, pits, and tooth-like projections on one side fit into their counterparts on the other side (≥ 2) (Flugel 2010). Different types in size and shape of stylolite are visited in the Jamal Formations. Stylolites are mostly found within the packstone-to-grainstone facies of shoal environment. They predominantly enjoy the zig-zag form and change facies fabrics. In the thin section, they frequently cross the entire rock and cut grains and matrix (Fig. 8e). Stylolite is formed on lithified sedimentary rocks during deep burial (Alsharhan and Whittle 1995).

Fracturing

Fractures are discrete breaks within a rock mass and comprise microfractures, joints, and faults. Many carbonate rocks display millimeter-to-centimeter-sized, mineral-filled (often calcite-filled) microfractures (Flugel 2010). In the thin sections, fractures and veins do not exhibit a certain order and can be found either individually or in groups. Two generations of fracturing can be seen in the facies, implying that an early fracture is filled and then intersected by a new one. These fractures are of fracturing and microfracturing types, which are closed and filled by microcrystalline calcite cement and dolomite (Fig. 8f). The Jamal Formation fractures are caused by tectonic stresses (from small scale to regional scale).

Paragenesis (diagenetic history)

According to petrographic studies, diagenetic processes of the Jamal Formation evolve in various digenetic environments including marine, meteoric, and burial diagenetic environments (Fig. 9). Marine environments' features involve micritization, bioturbation, physical compaction,

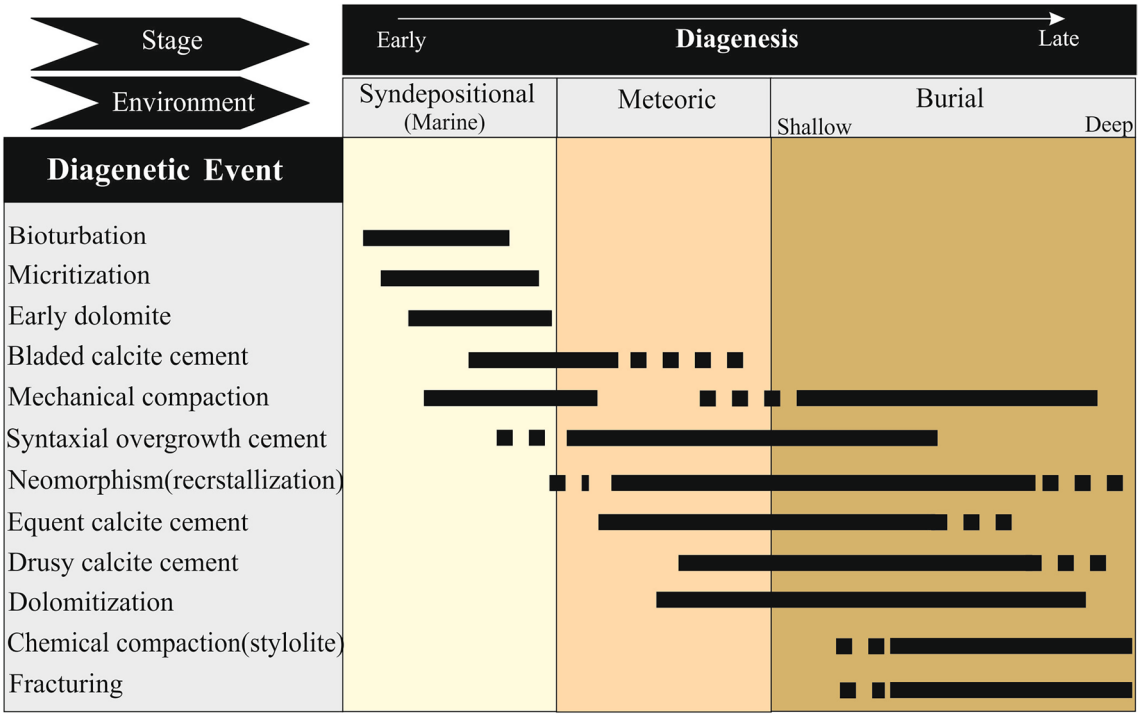

Fig. 9 Paragenetic sequence of carbonate Jamal Formation illustrating the diagenetic history of the main diagenetic features. The major diagenetic environments are marine, meteoric, and burial diagenetic environments, respectively

and bladed calcite cement. Neomorphism, syntaxial overgrowth, and equant calcite cement and dolomitization (fabric retentive dolomite) are the major meteoric processes. The main burial environment processes are dolomitization (fabric destructive dolomite), physical and chemical compaction, drusy calcite cement, and fracturing.

Conclusion

The Permian Jamal Formation of the Tang-e Sarve area (Central Iran) is a shallow water carbonate sequence and is composed of 11 microfacies that are belonged to shoal, lagoon, and tidal flat environments. These microfacies deposited on the on a shallow carbonate ramp (homoclinal ramp) with the gentle slope. Facies frequency analysis indicated that the lagoon environment has the highest abundance (48%) and tidal flat environment shows the least abundance of facies (17%). Bioturbation, micritization, cementation, dolomitization, neomorphism, physical and chemical compaction, and fracturing are the main diagenetic features that are created in the marine, meteoric, and burial diagenetic environments.

Acknowledgements The Department of Geology, Science and Research Branch, Islamic Azad University, Tehran, Iran supported this study.

References

Aghanabati A (1977) Etudgeologique de la region de Kalmard (W. Tabas). Geological Survey of Iran, Iran, pp 51–63

Aghanabati A (2004) Geology of Iran: Tehran. Geol Surv Iran 586:19–30 **(in Persian)**

Alavi M (1991) Sedimentary and structural characteristics of the Paleo-Tethys remnants in northeastern Iran. Geol Soc Ame Bull 103:983–992

Alavi M, Vazir H, Seyed-Emami K, Lasemi Y (1997) The Triassic and associated rocks of the Nakhlak and Aghdarband areas in central and northeastern Iran as remnants of the southern Turanian active continental margin. Geol Soc Am Bull 109:1563–1575

Aleali M, Rahimpour-Bonab H, Moussavi-Harami R, Jahani D, Asadi-Eskandar A (2013) Depositional environment and sequence stratigraphy of the Kangan Formation in South Pars field. Geosciences 22:65–74

Alsharhan AS, Whittle L (1995) Carbonate-evaporite sequences of the Late Jurassic—southern and southwestern Arabian Gulf. AAPG Bull 79:1608–1630

Alsharhan AS, Kendall CG, St C (2003) Holocene coastal carbonates and evaporites of the southern Arabian Gulf and their ancient analogue. Earth Sci Rev 61:191–243

Arefifard S, Davydov VI (2005) Petrography and geochemistry of Permian Strata in Tabas and Kalmard regions, Eastern-Central Iran. Geophys Res Abstr 7(00484):2005

Arefifard S, Isaacson P (2009) Microbiostratigraphy of Permian deposits in central Iran. EGU General Assembly conference, 19–24 April, 2009, Vienna, Austria, p 1699

Arefifard S, Isaacson PE (2011) Permian sequence stratigraphy in east-central Iran: microplate records of Peri-Tethyan and Peri-Gondwanan events. Stratigraphy 8(1):61–83

Bachmann M, Hirsch F (2006) Lower Cretaceous carbonate platform of the eastern Levant (Galilee and the Golan Heights): stratigraphy and second-order sea-level change. Cretac Res 27:487–512

Bathurst RGC (1966) Boring algae, micrite envelopes and lithification of molluscan biosparites. Geol J 5:15–32

Bathurst RGC (1989) Early diagenesis in carbonate sediments. In: Parker A, Sellwood BW (eds) Sediment diagenesis. Reidel, Dordrecht, pp 345–377

Bosence DWJ, Gibbons KA, Le Heron DP, Morgan WA, Pritchard T, Vining BA (2015) Microbial carbonates in space and time: implications for global exploration and production. Geol Soc Lond Spec Publ 418:1–15

Bottjer DJ, Droser ML (1994) The history of Phanerozoic bioturbation. In: Donovan SK (ed) Palaeobiology of trace fossils. Wiley, Chichester, pp 155–176

Brandano M, Frezza V, Tomassetti L, Pedley M (2010) Facies analysis and paleoenvironmental interpretation of the Late Oligocene Attard member (Lower Coralline Limestone Formation), Malta. Sedimentology 56:1138–1158

Bricker OP (1973) Carbonate cements. John Hopkins University Studies in Geology, Baltimore, pp 19–376

Bromley RG (1994) The palaeoecology of bioerosion. In: Donovan SK (ed) The paleobiology of trace fossils. Belhaven, London, pp 133–154

Bromley RG (1996) Trace fossils: biology, taphonomy and applications, 2nd edn. Kluwer, Dordrecht

Brunet MF, Granath JW, Wilmsen M (2009) South Caspian to Central Iran basins. Geol Soc Lond Spec Publ 312:1–6

Burchette TP, Wright VP (1992) Carbonate ramp depositional systems. In: Sellwood BW (ed) Ramps and Reefs. Sedimentary Geology, vol 79. Elsevier, Amsterdam, pp 3–57

Choquette PW, James NP (1987) Diagenesis, 12, Diagenesis in limestones, 3, The deep burial environment. Geosci Can 14:3–35

Davidov V, Arefifard S (2007) Permian fusulinid fauna of Peri-Gondwana affinity from the Kalmard region, east-central Iran and its significance for tectonics and paleogeography. Palaeontol Electron 10(2):40

Demicco RV, Hardie LA (1994) Sedimentary structures and early diagenetic features of shallow marine carbonate deposits, vol 1. SEPM, USA, p 265

Dercourt J, Ricou LE, Vriel Ynck B (1993) Atlas Tethys paleoenvironmental Maps. Gauthier-Villars, Paris, p 307

Dunham RJ, (1962) Classification of carbonate rocks according to depositional texture. In: Ham ED (ed) Classification of carbonate rocks: A Symposium: American Association of Petroleum Geologists. Memoir 1, 108–121

Embry AF, Klovan JE (1971) A late Devonian reef tract on Northeastern Banks Island, Northwest Territories. Bull Can Pet Geol 19(4):730–781

Ernst A, Senowbari-Daryan B, Hamedani A (2006a) Middle Permian Bryozoa from the Lakaftari area, central Iran. Geodiversitas 28:543–590

Ernst A, Senowbari-Daryan B, Rashidi K (2006b) Lower Permian Bryozoa of the Jamal Formation from Bagh-e Vang (Shotori Mountains, northeast Iran). Facies 52:627–635

Ernst A, Senowbari-Daryan B, Rashidi K (2008) Permian Bryozoa from the Jamal Formation of Shotori mountains (northeast Iran). Rev Paleobiol 27(2):395–408

Ernst A, Senowbari-Daryan B, Rashidi K (2009a) Rhabdomesid and cystoporid bryozoans from the Permian of Deh-e Mohammad, Shotori mountains (northeastern Iran). Geobios 42(2):133–140

Ernst A, Senowbari-Daryan B, Rashidi K (2009b) Bryozoa from the Surmaq Formation (Permian) of the Hambast mountains, south of Abadeh, central Iran. Facies 55:595–608

Flugel E (2010) Microfacies analysis of limestone: analysis. Springer, Berlin, p 976

Flügel E (1991) Triassic and Jurassic marine calcareous algae: a critical review. In: Riding R (ed) Calcareous algae and stromatolites. Springer, Berlin, pp 481–503

Geel T (2000) Recognition of stratigraphic sequences in carbonate platform and slope deposits: empirical models based on microfacies analysis of Paleogene deposits in southeastern Spain. Paleogeogr Palaeoclimatol Palaeoecol 155:211–238

Harris PM, Kendall CG, St C, Lerche J (1985a) Carbonate cementation: a brief review. In: Schneidermann M, Harris PM (eds) Carbonate cements. Society of Economic Paleontologists and Mineralogists, Tulsa, pp 79–95

Harris PM, Moore CH, Wilson JL (1985b) Carbonate depositional environments. Modern and ancient. Part 2: carbonate platforms, vol 80. Colorado School of Mines Quart, USA, pp 1–60

Hessami K, Nilforoushan F, Talbot CJ (2006) Active deformation within the Zagros mountains deduced from GPS measurements. J Geol Soc 163:143–148

Hird K, Tucker ME (1988) Contrasting diagenesis of two Carboniferous oolites from South Wales: a tale of climatic influence. Sedimentology 35:587–602

James NP (1991) Diagenesis of carbonate sediments, notes to accompany a short course. Geological Society of Australia, p 101

James NP, Choquette PW (1983) Diagenesis 6 limestone: the sea floor digenetic environment. Geosci Can 10:162–179

James NP, Choquette PW (1990a) Limestones—the meteoric diagenetic environment. In: Morrow DW (ed) Macillreath IA, vol 11. Diagenesis Geoscience Canada, Canada, pp 161–194

James NP, Choquette PW (1990b) Limestones—the burial diagenetic environments. In: Macillreath IA, Morrow DW (eds) Diagenesis, vol 4. Geoscience Canada Reprint, Canada, pp 75–111

James NP, Jones B (2015) Origin of carbonate sedimentary rocks. American Geophysical Union, Washington, p 464

Jenny-Deshusses C (1983) Le Permian de l´Elborz Central et Oriental (Iran): Stratigraphie et micropaleontologie (Foraminifères et Algues). Unpubl. These, no. 2130, University de Geneva, Section des sciences de la terre, Geneva, p 265

Jones SJ (2015) Introducing sedimentology. Dunedin Academic Press, Edinburgh, p 96

Kahler F (1974) Iranische Fusuliniden, vol 117. Jahrbuch für Geologie, Wien, pp 75–107

Kahler F (1977) Fusuliniden aus der Mediterranische-Iranische Gebiet. Neues Jahrbuch fûr Geologie und Paleontologie 4:199–216

Kendall AC (1975) Post-compactional calcitization of molluscan aragonite in a Jurassic limestone from Saskatchewan, Canada. J. Sediment Petrol 45:399–404

Kobluk DR, Risk MJ (1977) Calcification of exposed filaments of endolithic algae, micrite envelope formation and sediment production. J Sediment Petrol 47:517–528

Korngreen D, Benjamini C (2010) The epicontinental subsiding margin of the Triassic in Northern Israel, North Arabian Plate. Sediment Geol 228:14–45

Lasemi Y, Jahani D, Amin-Rasouli H, Lasemi Z (2012) Ancient carbonate tidalites. In: Davis RA, Dalrymple RW (eds) Principles of tidal sedimentology. Springer, Heidelberg, pp 567–607

Leven E Ja, Taheri A (2003) Carboniferous-Permian stratigraphy and fusulinids of East Iran. Gzhelian and Asselian deposits of the Ozbak-Kuh region. Riv Ital Paleontol Stratigr 109:21–38

Leven E Ja, Vaziri Moghaddam H (2004) Carboniferous–Permian stratigraphy and fusulinids of eastern Iran, The Permian in the Bagh-e- Vang section (Shirgesht area). Riv Ital Paleontol Stratigr 110:441–465

Leven EJA, Gorgij MN (2006) Upper Carboniferous-Permian stratigraphy and fusulinids from the Anarak region, central Iran. Russ J Earth Sci 8:25

Logan BW, Rezak R, Ginsburg RN (1964) Classification and environmental significance of algal stromatolites. J Geol 72:68–83

Longman MW (1980) Carbonate diagenetic textures from near surface diagenetic environments. Am Assoc Petrol Geol Bull 64:461–487

Maliva RG (1995) Recurrent neomorphic and cement microtextures from different diagenetic environments, quaternary to late neogene carbonates, Great Bahama Bank. Sediment Geol 97:1–7

Meyers WJ (1991) Calcite cement stratigraphy: an overview. In: Barker CE, Kopp OC (eds) Luminescence microscopy and spectroscopy: qualitative and quantitative applications, vol 25. SEPM Short Course, USA, pp 133–148

Middleton GV, Church MJ, Coniglio M, Hardie LA, Longstaffe FJ (2003) Encyclopedia of sediments and sedimentary rocks. Springer, Netherlands, p 821

Moore CH (1989) Carbonate diagenesis and porosity. Elsevier, Amsterdam, p 338

Moore CH, Wade WJ (2013) Carbonate reservoirs: porosity, evolution and diagenesis in a sequence stratigraphic framework: porosity evolution and diagenesis in a sequence stratigraphic framework, 2nd edn. Elsevier, Amsterdam, p 369

Mousavi SM (2017) Mapping seismic moment and b-value within the continental-collision orogenic-belt region of the Iranian Plateau. J Geodyn 103(2017):26–41

Naimi-Ghassabian N, Khatib MM, Nazari H, Heyhat MR (2015) Present-day tectonic regime and stress patterns from the formal inversion of focal mechanism data, in the North of Central-East Iran Blocks. J Afr Earth Sci 111:113–126

Nogole sadat MA (1978) Les zones de decrochement et les virgations structurales en Iran. Consequences des resultants de l'analyse structurales de la region de Qom. Unpubl. Ph. D. Thesis, University Scientifique et Medicate de Gernoble, p 201

Palma RM, Lopez- Gomez J, Piethe RD (2007) Oxfordian ramp system (La Manga formation) in the Bardas Blances area (Mendoza Province) Neuquen Basin Argentina: facies and depositional sequences. Sedimentary Geology 195:113–134

Partoazar H (1992) Changsingian stage in east Iran. Discovery of genus Colaniella and its biostratigraphic importance. Geol Surv Iran Geosci Period 3:44–53 **(in Farsi with English abstract)**

Partoazar M (1995) Permian deposits in Iran. Geol Surv Iran 22:340 **(in Persian)**

Partoazar M, Hamdi B, Aghanabati SA (2014) New approach on biostratigraphy of Permian deposits of Jamal formation in Bagh Vang section, Shirgesht area (Central Iran). Geopersia 4(2):141–154

Patterson WP, Walter LM (1994) Syndepositional diagenesis of modern platform carbonates: evidence from isotopic and minor element data. Geology 22:127–130

Pierson BJ, Shinn EA (1985) Cement distribution and carbonate mineral stabilization in Pleistocene limestones of Hogsty Reef, Bahamas. In: Schneidermann N, Harris PM (eds) Carbonate cements, Special Publication 36. Society of Economic Paleontologists and Mineralogists, Tulsa, pp 153–168

Pingitore NE (1976) Vadose and phreatic diagenesis: processes, products and their recognition in corals. J Sediment Petrol 46:985–1006

Pomar L (2001) Types of carbonate platforms: a genetic approach. Basin Res 13:313–334

Pratt BR (2010) Peritidal carbonates. In: James NP, Dalrymple RG (eds) Facies models, 3rd edn. Geological Association of Canada, St. John's **(in press)**

Rankey E, Berkeley A (2012) Holocene carbonate tidal flats. In: Davis RA Jr, Dalrymple RW (eds) Principles of tidal sedimentology. Springer, Netherlands, pp 507–535
Rashidi K, Senowbari-Daryan B (2010) Dasycladales from the Permian Jamal Formation of Shotori mountains, northeast Iran. Facies 56:111–137
Read JF (1985) Carbonate platform facies models. Am Assoc Pet Geol Bull 69:1–21
Reid RP, Macintyre IG, Post JE (1992) Micritized skeletal grains in northern Belize lagoon: a major source of Mg–calcite mud. J Sediment Petrol 62:145–156
Reilinger R, McClusky S, Vernant P, Lawrence S (2006) GPS constraints on continental deformation in the Africa–Arabia–Eurasia continental collision zone and implications for the dynamics of plate interactions. J Geophys Res 111:B05411. https://doi.org/10.1029/2005JB004051
Riding R (1999) The term stromatolite: towards an essential definition. Lethaia 32:321–330
Riding R (2000) Microbial carbonates: the geological record of calcified bacterial–algal mats and biofilms. Sedimentology 47:179–214
Rigby JK, Senowbari-Daryan B, Hamedani A (2005) First reported occurrence of wewokellid sponges (Calcarea, Heteractinida) from the Permian of central Iran. Facies 51:516–521
Ruban DA, Al-Husseini MI, Iwasaki Y (2007) Review of Middle East Paleozoic plate tectonics. GeoArabia 12(3):35–56
Rutner A, Nabavi M, Hajian J (1968) Geology of the shirgesht area (Tabas area, East Iran), Tehran. Geol Surv Iran Rep 4:133
Sandberg P (1985) Aragonite cements and their occurrence-in ancient limestones. In: Schneidermann N, Harris PM (eds) Carbonate cements, vol 36. Society of Economic Paleontologists and Mineralogists, Tulsa, pp 33–58
Schneidermann N, Harris PM (1985) Carbonate cements, vol 36. Society of Economic Paleontologists and Mineralogists, Tulsa, p 397
Scoffin TP (1988) The environments of production and deposition of calcareous sediments on the shelf west of Scotland. Sediment Geol 60:107–134
Scotese CR, Langford RP (1995) Pangea and the paleogeography of the Permian. In: Scholl PA, Peryt TM, Ulmer-Scholl DS (eds) The Permian of Northern Pangea. Springer, Berlin, pp 3–19
Sengor AC (1984) The Cimmeride orogenic system and the tectonics of Eurasia. Boulder Geol Soc Am Spec Pap 19:82
Senowbari-Daryan B, Hamedani A (2002) First report of the occurence of Amblysiphonella, a thalamid sponge from the Permian of Iran and description of *A. iranica* n. sp. from central Iran. Rev Paleobiol Genève 21(2):795–801
Senowbari-Daryan B, Rashidi K (2010) The codiacean genera Anchicodium Johnson, 1946 and Iranicodium nov. gen. from the Permian Jamal Formation of Shotori mountains, northeast Iran. Rivista Italiana di Paleontologia e Stratigraphia 116(1):3–21
Senowbari-Daryan B, Rashidi K (2011) Lercaritubus Problematicus Flugel, Senowbari-Daryan and di Stefano and Vangia Telleri (Flugel): two problematic organisms from the Permian Jamal Formation of Shotori mountains, northeast Iran. Rivista Italiana di Paleontologia e Stratigrafia 117(1):105–114
Senowbari-Daryan B, Rashidi K, Hamedani A (2006) Sponge assemblage of the Permian reefal limestones of Kuh-e Bagh-e Vang, Shotori mountains (East Iran). Geol Carp 56(6):381–406
Senowbari-Daryan B, Hamedani A, Rashidi K (2007) Sponges from the permian of hambast mountains, south of Abadeh, Central Iran. Facies 53(4):575–614
Senowbari-Daryan B, Rashidi K, Saberzadeh B (2011) Dasycladalean green algae and some problematic algae from the Upper Triassic of the Nayband Formation (northeast Iran). Geol Carpa 62(6):501–517
Shinn EA (1968) Burrowing in recent lime sediments of Florida and the Bahamas. J Palaeontol 42:879–894
Shinn EA (1983) Tidal flat environment. In: Scholle PA, Bebout DG, Moore CH (eds) Carbonate depositional environments. American Association Petroleum Geologists, Tulsa, pp 173–210
Shinn EA (1986) Modern carbonate tidal flats: their diagnostic features, vol 81. Colorado School of Mines Quarterly, Colorado, pp 7–35
Sotohian F (2016) Microfacies and sequence stratigraphy of the Permian rocks in Kuh-Jamal section (Tabas). J Curr Res Sci 1:477–486
Stocklin J (1977) Structural correlation of the Alpine ranges between Iran and Central Asia. Memoires hors-series de la Societé géologique de France 8:333–353
Stocklin J, Nabavi MH (1969) Geologic map of the Boshruyeh, Scale 1:250 000, No. J7. Geological Survey of Iran
Stocklin J, Eftekhar-Nezhad J, Hushmand-Zadeh A (1965) Geology of the Shotori range (Tabas area, East Iran). Geol Surv Iran Rep 3:69 **(in Persian)**
Taheri A (2002) Stratigraphy of Permian sediments in Tabas area. Ph.D. thesis, Univ. Isfahan, p 157 **(in Persian)**
Takin M (1972) Iranian geology and continental drift in the Middle East. Nature 235:147–150
Torsvik TH, Cocks LRM (2004) Earth geography from 400 to 250 Ma: a palaeomagnetic, faunal and facies review. J Geol Soc Lond 161:555–572
Tucker ME (2001) Sedimentary petrology, 3rd edn. Blackwell, Oxford, p 262
Tucker ME, Bathurst RGC (1990) Carbonate diagenesis. Int Assoc Sedimento Repr Ser 1:312
Tucker ME, Wright VP (1990) Carbonate sedimentology. Blackwell, Oxford, p 482
Warren JK (2006) Evaporites: sediments, resources and hydrocarbons: Springer, Berlin, p 1041
Wilson JL (1975) Carbonate facies in geological history. Springer, Berlin, p 471
Wray JL (1977) Calcareous algae. Elsevier, New York, p 185
Yarahmadzahi H (2011) Fusulinids biostratigraphy and sequence stratigraphy of Lower Permian deposits in Central Iran (Isfahan, Shareza, Abadeh and Yazd areas), PhD thesis, Science and Research Branch, Islamic Azad University, Tehran, Iran (in Persian)